Applied Geography 157 (2023) 103017

Contents lists available at ScienceDirect

Applied Geography

journal homepage: www.elsevier.com/locate/apgeog

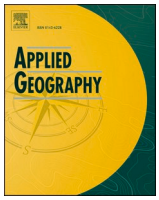

Social and environmental vulnerability to flooding: Investigating cross-scale hypotheses

Selena Hinojos [a], Lauren McPhillips [b], Peter Stempel [c], Caitlin Grady [a,*]

[a] Department of Engineering Management and Systems Engineering, The George Washington University, Washington, DC, USA
[b] Departments of Civil and Environmental Engineering, Agricultural and Biological Engineering, The Pennsylvania State University, University Park, PA, USA
[c] Department of Landscape Architecture, The Pennsylvania State University, University Park, PA, USA

ARTICLE INFO

Handling Editor: J Peng

Keywords:
Flooding
Social vulnerability
Index
Scale
Natural hazard
MAUP
Modifiable areal unit problem
SOVI
Flood exposure
Indicators
Social equity

ABSTRACT

Flooding is a natural hazard that touches nearly all facets of the globe and is expected to become more frequent and intensified due to climate and land-use change. However, flooding does not impact all individuals equally. Therefore, understanding how flooding impacts distribute across populations of different socioeconomic and demographic backgrounds is vital. One approach to reducing flood risk on people is using indicators, such as social vulnerability indices and flood exposure metrics, to inform decision-making for flood risk management. However, such indicators can face the scale and zonal effect produced by the Modifiable Areal Unit Problem (MAUP). This study investigates how the U.S. Census block group, tract, and county scale selection impacts social vulnerability and flood exposure outcomes within coastal Virginia, USA. Here we show how (1) scale selection can obstruct our understanding of drivers of vulnerability, (2) increasingly aggregated scales significantly undercount highly vulnerable populations, and (3) hotspot clusters of social vulnerability and flood exposure can identify variable priority areas for current and future flood risk reduction. Study results present considerations about using such indicators, given the real-life consequences that can occur due to the MAUP. The results of this work warrant understanding the implications of scale selection on research methodological approaches and what this means for practitioners and policymakers that utilize such information to help guide flood mitigation strategies.

1. Introduction

Flooding is a near-ubiquitous natural hazard faced globally. The frequency and extent of flooding impacts on the interconnected natural, social, economic, and built environment are projected to rise due to accelerated climate and land-use change. The United States, in 2021 alone, endured six billion-dollar flooding and tropical cyclone events (NCEI, 2022). The risk of flooding, or the product of flood exposure, hazard, and vulnerability (Qiang et al., 2017), from such events is unequally experienced across socioeconomic and demographic groups (Gourevitch et al., 2022). Hazard and environmental justice scholars have demonstrated clear patterns of flooding inequities faced by people of color and lower-income populations in the U.S. (Mazumder et al., 2022), for example (Chakraborty et al., 2014; Collins et al., 2019; Linscott et al., 2022). Inequitable social conditions such as marginalizing policies, systematic deprivation of resource access, placement within flood-prone areas, and poor infrastructure have disproportionately impacted underserved and underestimated communities. Such conditions enhance these social groups' vulnerabilities by decreasing their ability to prepare financially, respond to the threat of an imminent flood event, and recover from a flood if implicated (Cutter et al., 2003).

Practitioners and policymakers widely utilize index-based measures to quantify hard-to-measure social vulnerabilities (Rufat et al., 2019). Scholars acknowledge the utility of understanding the landscape of social vulnerability to help guide natural hazard risk reduction planning and recovery, despite criticisms about certain shortcomings like sensitivity to selected indicators (Spielman et al., 2020). One widely used index within hazards literature is the "hazard-of-place" Social Vulnerability Index (SoVI) (Cutter et al., 2003), a data-driven quantitative method and theoretical framework used to understand a community's relative sensitivity and adaptive capacity to natural hazards (Gu et al., 2018; Spielman et al., 2020). SoVI embeds epistemic uncertainty (Tate, 2013), one ambiguity being the 'scale' (size) of areal units being analyzed, which is essential in vulnerability assessments (Fekete et al.,

* Corresponding author. 800 22nd St NW, Washington, DC, 20052, USA.
E-mail address: Caitlin.grady@gwu.edu (C. Grady).

https://doi.org/10.1016/j.apgeog.2023.103017
Received 13 February 2023; Received in revised form 22 May 2023; Accepted 10 June 2023
Available online 14 June 2023
0143-6228/

2010). Scale selection is a multifaceted decision based on the factors such as project objectives and the intended end-use. However, the selection of scale and whether such selection has unintended consequences remains an underexplored area of literature.

Although multiple studies explore the uncertainty and sensitivity of SoVI construction (Schmidtlein et al., 2008; Tate, 2013), such as indicator selection (e.g., Spielman et al., 2020), limited studies investigate how scale impacts the outcome of index-based measures for flood risk results. Many studies explore flood vulnerabilities at different scales, such as the Census block group (BG) (Pricope et al., 2019), tract (Shao et al., 2020; Tate et al., 2021; Y (Victor) Wang & Sebastian, 2021), and county scale (Khajehei et al., 2020). However, there are limited multi- and cross-scale studies investigating vulnerabilities to flooding (Remo et al., 2016). Two U.S.-based multi-scale flood vulnerability studies revealed that finer spatial scales had identified more vulnerable communities overlooked at larger spatial scales (e.g., block-level vs. tract) (Remo et al., 2016; Tanir et al., 2021).

SoVI or any other index or analysis embeds socioeconomic and demographic data that has aggregated point data at certain scales, which can result in the unsolved spatial analysis phenomenon called the Modifiable Areal Unit Problem (MAUP). The MAUP occurs when selecting aerial units based on identical data can alter the analytical results (Fotheringham & Wong, 1991; Openshaw, 1984). The MAUP can arise by modifying a unit's size or shape, referred to as the scale and zonation effect. The scale effect occurs based on the size of the aggregation. For decreased levels of aggregation or greater areal units, the correlations between the variables tend to decrease while the variation increases, given that the data's extremes are more dominant than with lesser areal units (Fotheringham & Wong, 1991; Openshaw & Taylor, 1979). Whereas the zoning effect occurs based on the shape or configuration of the system across geographic space (Fotheringham & Wong, 1991). These effects of the MAUP can regroup data observation into infinite arrangements, effectively producing new summary values that alter the understanding of that observation (Buzzelli, 2020). To the extent that indices like SoVI rely on Census data that does not use standardized areal units, they are subject to the MAUP.

This research seeks to address the knowledge gap in understanding and applying indices of social vulnerability and flood risk. Utilizing the case study area of coastal Virginia, we address the following research questions: 1) How does scale influence social correlates of the SoVI indicators within coastal VA? 2) Where does high and low social vulnerability coincide with flood exposure in coastal VA? How does this vary across scales? 3) What implications does this raise for researcher methods? We aim to explore how the MAUP and the selection of scale (e.g., BG, tract, county) impact outcomes relating to SoVI and flood risk. Our findings could guide future decision-making about scale selection within flood vulnerability quantification. Furthermore, they could provide insight into managing hazard risk equitably, thereby reducing the risk of floods on communities.

2. Materials and methods

2.1. Study area

The site of investigation for our work is coastal VA, a historically rich and socially complex region that encompasses around 6 million people, around 70% of the state's population (Bureau, 2020; VA Dept. of Cons. and Rec, 2021). These Virginians face unprecedented coastal and inland flooding pressures from changing precipitation patterns and containing areas with the second largest population centers at risk of sea level rise in the U.S. (NOAA, 2023). The flood risk that these communities face is extreme. For example, by 2080, there is an expected 180% increase in the number of residents exposed to coastal flooding – around 943,000 people (VA Dept. of Cons. and Rec, 2021). This low-lying region is also highly vulnerable to economic, environmental, and cultural loss, with 250,000 acres of land just under 5 feet above the high tide line (Strauss et al., 2014). Nearly 9.3% of coastal Virginians face poverty, of which 13.2% fall within the 2020 floodplain, making this site a prime area for a social vulnerability and flood exposure investigation (VA Dept. of Cons. and Rec, 2021).

Within coastal VA, there are eight Planning District Commissions (PDCs) and Regional Commissions (RCs), which are political subdivisions of voluntary associations of the local government. These commissions bridge intergovernmental cooperation, determine common needs, study regional issues, and determine cost-saving viable solutions, among other obligations (VA Dept. of Cons. and Rec, 2021). The geographical boundaries of the commissions encompass four master planning regions: Fall Line North, Fall Line South, Hampton Roads, and Rural Coastal VA. These regions are actively utilized for the Virginia Coastal Resilience Master Plan, which is a call to action for the Commonwealth to protect and foster an equitably resilient coast for all Virginians. Therefore, to bridge policy relevance, the BGs, tracts, and counties within the boundaries of the commissions were used for this study (Fig. 1) (See supplementary section S.1 for additional spatial features of coastal VA).

2.2. Research design

We used socioeconomic and demographic information, land cover, and 100-year floodplain data across BG, tract, and county scales to investigate the spatial relationships between social vulnerability and flood exposure across these scales in coastal VA. Fig. 2 summarizes the three methodological elements used. First, we produced three social vulnerability indices (SoVIs) using principal component analysis (PCA). The SoVIs were generated at the BG, tract, and county scale based on the Census Bureau's 2019 American Community Survey (ACS). Then, we developed three flood hazard exposure metrics (HEMs) by combining the 2019 National Land Cover Database (NLCD) land cover data with the Federal Emergency Management Agency (FEMA) 100-year flood hazard data through a dasymetric mapping technique, following the approach of Tate et al. (2021). The HEMs are the percent of habitable areas that are flood exposed per BG, tract, or county. Collectively, the HEMs and SoVIs were spatially analyzed using a bivariate Local Indicators of Spatial Association (LISA) approach to identify hotspots and outliers of spatial autocorrelation between social vulnerability and flood exposure. Lastly, we analyzed Moran's I coefficients to detect variable spatial patterns for the SoVIs, HEMs, and the spatial clusters of HEMs surrounded by SoVIs.

2.3. Social vulnerability index

We adapted the "hazards-of-place" model approach based on spatial vulnerability indicators from the latest edition of SoVI (Hazards and Vulnerability Research Institute, 2015) to measure the spatial distribution of social vulnerability to flooding (Cutter et al., 2003). This inductive model utilizes PCA to generate principal component (PC) factors that contain much of the variation among the set of indicators (Hotelling, 1933; Pearson, 1901). The factors are then aggregated to produce a composite SoVI score. We selected the SoVI and the PCA approach for this study based on its widespread adoption within vulnerability assessment frameworks (Abson et al., 2012; de Loyola Hummell et al., 2016; Rabby et al., 2019; Schmidtlein et al., 2011; Tasnuva et al., 2020; C. Wang & Yarnal, 2012) and for comparability purposes.

Twenty-nine socioeconomic, demographic, and ethnic indicators (Table 1) were extracted at the BG, tract, and county scale from the 2015–2019 U.S. Census ACS (US Census Bureau, 2019) for the SoVI analysis using the *tidycensus* R package (Walker, 2022). We selected these three scales for comparability objectives, uncertainty reduction, and maintaining indicator and temporal uniformity (Supplementary Section S.2).

In line with previous literature (HVRI, 2016), we completed standard

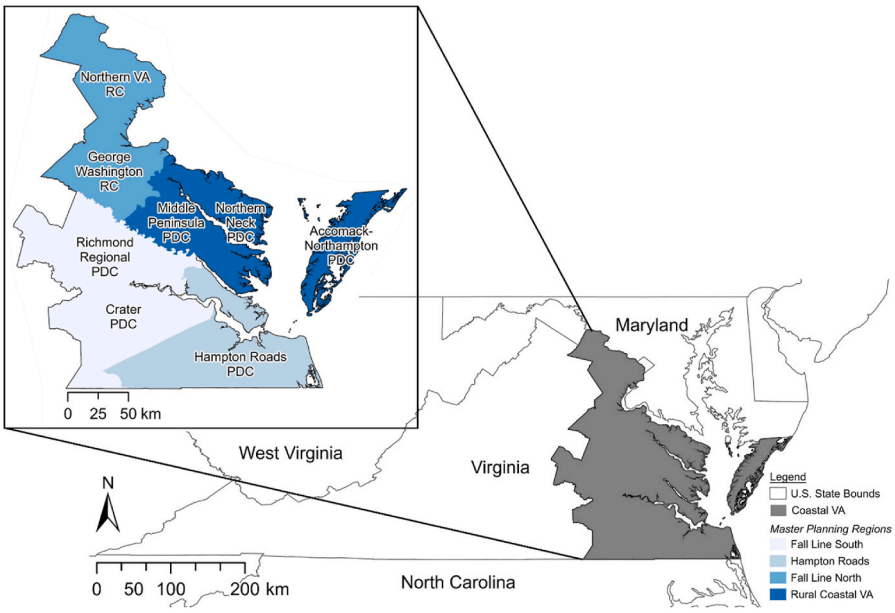

Fig. 1. Study site selection of Coastal Virginia and the Master Planning Regions encompassing the Planning District Commissions (PDCs) and Regional Commissions (RCs).

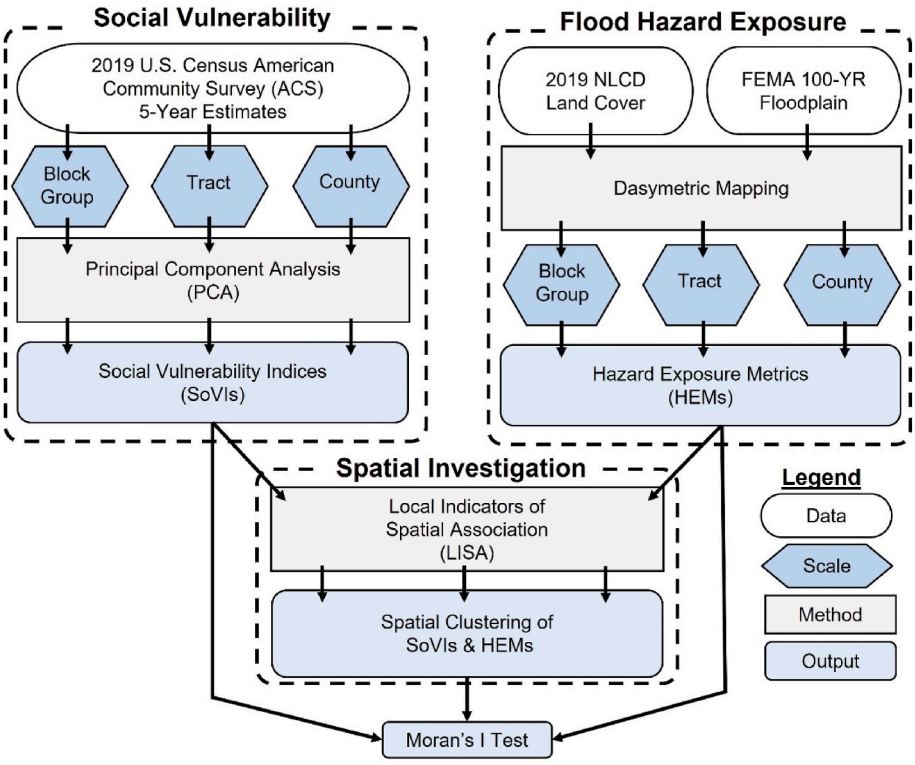

Fig. 2. Analytical framework of the study.

computation and normalization, verification of linearity and accuracy of the data, diagnostic testing, z-score standardization, eigenvalue-based Kaiser selection criterion, varimax rotation, and used an additive model to produce the SoVI scores (Equation (1)) (Supplementary Section S.3).

$$SoVI_{Score} = \Sigma\left[(\pm \, or \, \|) \, Factor_1 + ..(\pm \, or \, \|) \, Factor_X\right] \quad (1)$$

We spatially mapped the SoVI factor scores into six divergent classes based on the standard deviation from the mean to highlight the most and least vulnerable areal units per scale, ranging from −1.5 (lower vulnerability) to +2.5 (higher vulnerability). We utilized Python Version 3.9 to perform all SoVI analyses (see Supplementary Section S.4).

2.4. Flood hazard

To represent flood hazard, we utilized the FEMA National Flood Hazard Layer (NFHL) 100-year high-risk floodplain. The flood hazard

Table 1
The social vulnerability indicators utilized for the SoVI creation (Modified from Tate et al., 2021).

Category	Indicator	Indicator Code
Age	% Population <5 years & ≥ 65 years	UNDER5OVER65
	Median Age	MEDAGE
Education	% Less than 12th grade education	LIMEDU
Employment	% Employment in extractive industries	EMPEXT
	% Employment in service industries	EMPSER
Race	% Black or African American	BLACK
	% Asian	ASIAN
	% American Indian or Alaskan Native	AIAN
Ethnicity	% Hispanic	HISP
Family Structure	**% Children living in married coupled families**	CHILDMF
	% Female-headed households	FEMHH
	People per housing unit	HHDENSITY
Gender	% Female	FEM
	% Female participation in labor force	FEMLABFORCE
Health	% Population without health insurance	NOHEALTHINS
Housing	% Renters	RENTER
	% Rent burdened	RENTBUR
	Median gross rent	MEDRENT
	% Mobile homes	MOBHOME
	% Unoccupied housing units	VACANTHH
Wealth	**Median housing value**	MEDHHVALUE
	% Civilian unemployment	UNEMP
Income	% Poverty	POV
	% Households earning ≥ $200,000 annually	HH200k
	Per capita income	PERCAPINC
Dependence	% Households receiving social security	HHSSINC
	Nursing home residents per capita	NURSINGHPERCAP
Language	% Limited English proficiency	LIMENG
Mobility	% Housing unit with no car	NOTRANS

*A bolded indicator implies that an increase in the indicator results in a reduction of social vulnerability.

layers, representing fluvial (riverine) and coastal flood types, are available from the FEMA Flood Map Service Center (FEMA, 2022). The FEMA flood hazard data is scrutinized for the spatial (Qiang et al., 2017) and temporal scarcity (Birkland et al., 2003) within the U.S., as well as the ability to capture pluvial (rainfall-driven) flood hazards (NASEM, 2019); however, it has been the standard since 1968 in determining federal flood insurance and general community tactics to combat flooding risks (Blessing et al., 2017). We selected FEMA flood maps for this analysis given the high spatial resolution, the regularity for use in policy and regional development (Huang & Wang, 2020; Qiang, 2019b), and prevalence in guiding local planning (Huang & Wang, 2020).

To process these data, we disaggregated the NFHL county shapefiles into binary raster grids at a 30-m resolution at the BG, tract, and county scales. Each cell in the flood grid represented being within the 100-year floodplain (wet cell) or outside of the floodplain (dry or no-data cell). No-data classified cells are open-water areas. We conducted all hazard analyses in ArcGIS Pro Version 2.9.2.

2.5. Flood exposure

To measure people's exposure to flooding, we then calculated the relative area of habitability across scales using land cover data. Population exposure disaggregated based on land cover is one approach to measuring flood exposure (Debbage, 2019; Qiang, 2019a; Tate et al., 2021); however, there are several alternative methods of quantifying exposure that vary in accuracy and resolution, see (Crowell et al., 2010; Huang & Wang, 2020; Yager & Rosoff, 2017).

The land cover data is a 30-m resolution raster containing cells with 20 different land cover types categorized by the Anderson Land Cover Classification System (NLCD, 2019). Following the approach of Tate et al., 2021, we used the dasymetric categories of the EnviroAtlas map from the U.S. Environmental Protection Agency (EPA) to identify areas in which people are most likely to reside based on land type (Tate et al., 2021; US EPA, O., 2015). Based on the underlying assumption of the EnviroAtlas dasymetric population map, we assume the population is equally distributed, and land cover classes of open water, perennial ice/snow, and emergent herbaceous wetlands are considered uninhabitable land cover types. Habitable areas include developed, barren, forest, shrubland, herbaceous, planted/cultivated, and wetland land cover (Supplementary Section S.5). Habitability categories 1 through 5 were retained for this study, and non-habitable categories were removed. The sum of habitable cells per spatial scale from the binary raster of land cover acted as the denominator for the HEMs.

2.6. Hazard exposure metric

Combining flood hazard and flood exposure, we created hazard exposure metrics (HEMs) to measure areas within the floodplain in which people reside. We completed this by combining the FEMA flood hazard raster with the flood exposure habitable land cover raster through a dasymetric population mapping technique. Dasymetric mapping is a geospatial technique that can utilize land cover to distribute population data more accurately across a geographic boundary, such as BGs, tracts, and counties (US EPA, O., 2015). This technique has been applied in other flood exposure and risk analyses see (Debbage, 2019; Flores et al., 2023; Maantay & Maroko, 2009; Montgomery & Chakraborty, 2013; Qiang, 2019a; Tate et al., 2021; Wing et al., 2018).

Through a cell-by-cell stacked raster approach, we combined the habitable land use cells with the FEMA flood hazard cells. The sum of the habitable cells within the floodplain per BG, tract, and county was retained for the numerator of the HEMs. Finally, the ratio of flooded habitable cells to habitable cells across scales produces the HEMs (Equation (2)).

$$HEMs = \frac{\sum Habitable\ flood\ exposed\ areas\ (per\ areal\ unit)}{\sum Habitable\ areas\ (per\ areal\ unit)} \quad (2)$$

We then spatially mapped the resulting HEM scores into four divergent classes based on the standard deviation from the mean to highlight the most and least flood hazard-exposed geographical units, ranging from −0.5 (lower HEM) to +1.5 (higher HEM). Note that additional operations within ArcGIS Pro were necessary to create the HEMs (Supplementary Section S.6).

2.7. Spatial analysis of HEM and SoVI

We employed a bivariate LISA cluster mapping technique to examine the spatial relationship between the HEMs and the composite SoVIs scores at BG, tract, and county scale. The LISA approach identifies local patterns where data values present strongly positive spatial associations (clusters) or strongly negative spatial associations (outliers). We identified four types of LISA clusters and outliers by how flood hazard exposure values vary with social vulnerability values. 1) High-High (H–H), a geographic unit, and its neighboring units both ranked high in the HEM and SOVI. 2) Low-Low (L-L), a geographic unit, and its neighboring units both ranked low in the HEM and SOVI. 3) High-Low (H-L), HEM is ranked high in a geographic unit, while SoVI is ranked low in the neighboring units. 3) Low-High (L-H), HEM is ranked low in a geographic unit, while SoVI is ranked high in the neighboring units. GeoDa™ version 1.8 was utilized for the exploratory spatial analysis of LISA clusters (detailed LISA steps are outlined in Supplementary Section S.7).

3. Results

3.1. The effect of spatial scale on social vulnerability

We found that no indicators within the first PC factor F1 load consistently across scales (Fig. 3). This reveals that there is no leading

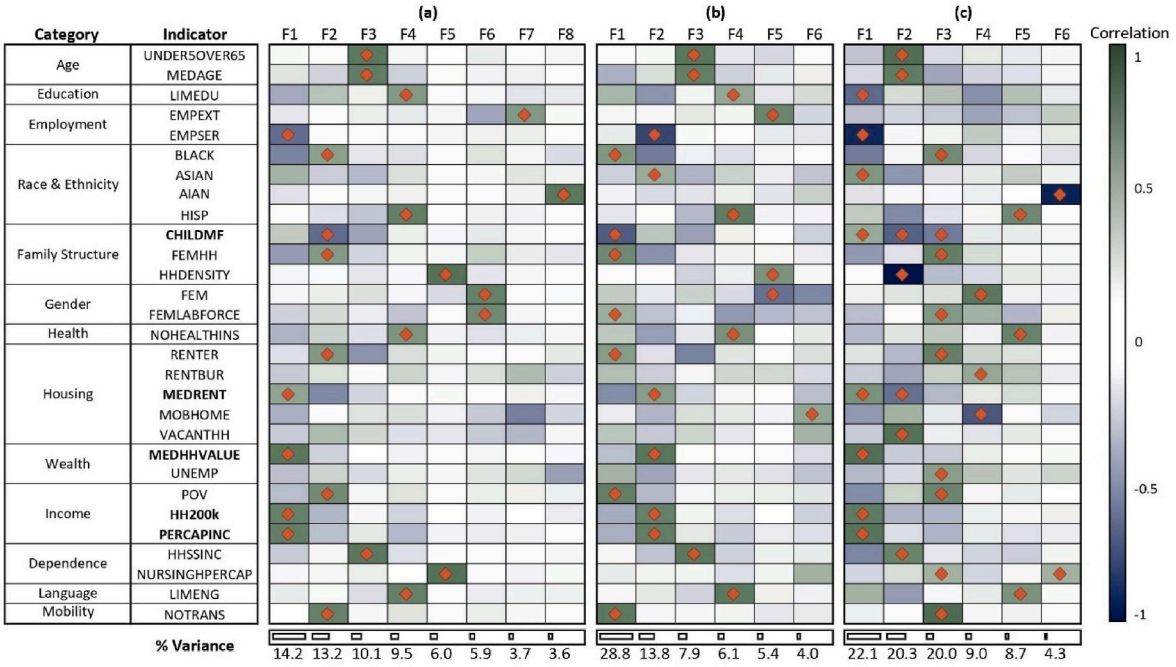

Fig. 3. The PC factor loadings (F) or correlation of indicators to social vulnerability (social correlates) at the (a) BG, (b) tract, and (c) county scale. The scale bar represents F's relative correlation (−1 to +1). The dominant indicator with a correlation greater than ±0.50 is characterized as a primary driver within that PC factor loading (F). The diamonds (◊) represent an indicator with a correlation ≥ ± 0.50. The percent variance explained by each F is displayed.

vulnerability indicator that transverses scales. We also found that the following eight indicators lack an explanation across two or more scales: employment in extractive industries, Asian, American Indian or Alaskan Native, rent burdened, mobile homes, unoccupied housing units, civilian unemployment, and nursing home residents per capita. Specifically, the eight indicators present significant prevalence in at least one scale but are generally the least influential in the model, loading on the PCs with the least variance.

Additionally, across the SoVIs, there are consistent themes that vary across PC factors. The following indicators are highly loading factors on PC F1, F2, or F3 across scales: employment in service industries, Black or African American, children living in married coupled families, female-headed households, renters, housing unit with no car, poverty, low values of median gross rent, median housing value, households earning ≥ $200,000 annually, and per capita income. Therefore, economic inequities, socially vulnerable demographic groups, and mobility challenges could be considered significant drivers of social vulnerability within coastal VA.

The PCA revealed dissimilarities in the dimensions of social vulnerability detected with scale. The variance explained by the vulnerability data at the BG, tract, and county scales is 66.1, 66.0, and 84.3 percent. This result suggests that the SoVI data is better explained at the county scale versus the less aggregated scales. The pooled summary results, including the number of PC factors, the associated indicators, general themes, and the individual and cumulative percent variance found at each scale, can be found in the Supplementary Section S.8.

The SoVI maps reveal that the finer aggregated BG and tract scales identify greater detailed areas of vulnerability that are not easily interpretable at the county scale (Fig. 4). Spatial trends show contrasting results between scales. A single geographical unit could be characterized as high vulnerability at one scale and featured as low vulnerability at another due to the MAUP.

We found that larger aggregated scales accounted for more people at lower SoVI levels, whereas less aggregated (finer spatial) scales reported more people at medium and high SoVI levels (Fig. 5). This result suggests that finer spatial scales could be valuable in detecting populations that could be neglected at greater aggregated scales.

3.2. The spatial pattern of flood hazard exposure

The spatial choropleth maps representing the HEMs show consistent spatial patterns with elevated flood exposure along the coastline, beginning at Virginia Beach, toward the Chesapeake Bay, and within the eastern shore of VA (Fig. 6). The increased exposure is an anticipated conclusion given the proximity to major inland and coastal water bodies. However, there are spatial differences in the HEMs based on the statistical subdivisions between scales. For example, the mean flood exposure within coastal VA at the BG, tract, and county scale as percent are 9.5, 10.3, and 12.2, respectively. Results exhibit an increase in mean flood exposure per areal unit with scale. This is an expected result, given that increased aggregated scales are likely to dampen the influence of extremes.

3.3. The spatial distribution of flood exposure and social vulnerability

Three bivariate (i) LISA cluster maps and (ii) cluster significance maps at the BG, tract, and county scale spatially identify local clusters and local spatial outliers of the HEMs surrounded by the SoVIs (Fig. 7). The significance maps show that the statistical significance of the individual clusters fluctuates greatly with scale. The spatial differences in the bivariate cluster maps were unexpected, given that the same foundational unaggregated data is utilized for SoVI and HEM creation. However, a consistent spatial trend across scales is areas of L-L occurring in northern coastal VA. Generally, spatial variability of statistically identified clusters decreases at the county scale; for example, H-L areas of vulnerability are not significant within coastal VA – which is not the case at the BG and tract scale. Following previous trends, smaller aggregated scales (BG and tract) provided greater detail on the landscape of flood exposure and social vulnerability.

From a flood risk reduction perspective, areas of variable flood exposure surrounded by high vulnerability (H–H and L-H) are target locations to prioritize. H–H locations are the most at risk, given elevated vulnerability and exposure. L-H areas could be considered high risk in the future with intensified flood events and alterations of the landscape. The difference across scale in population counts encompassing highly

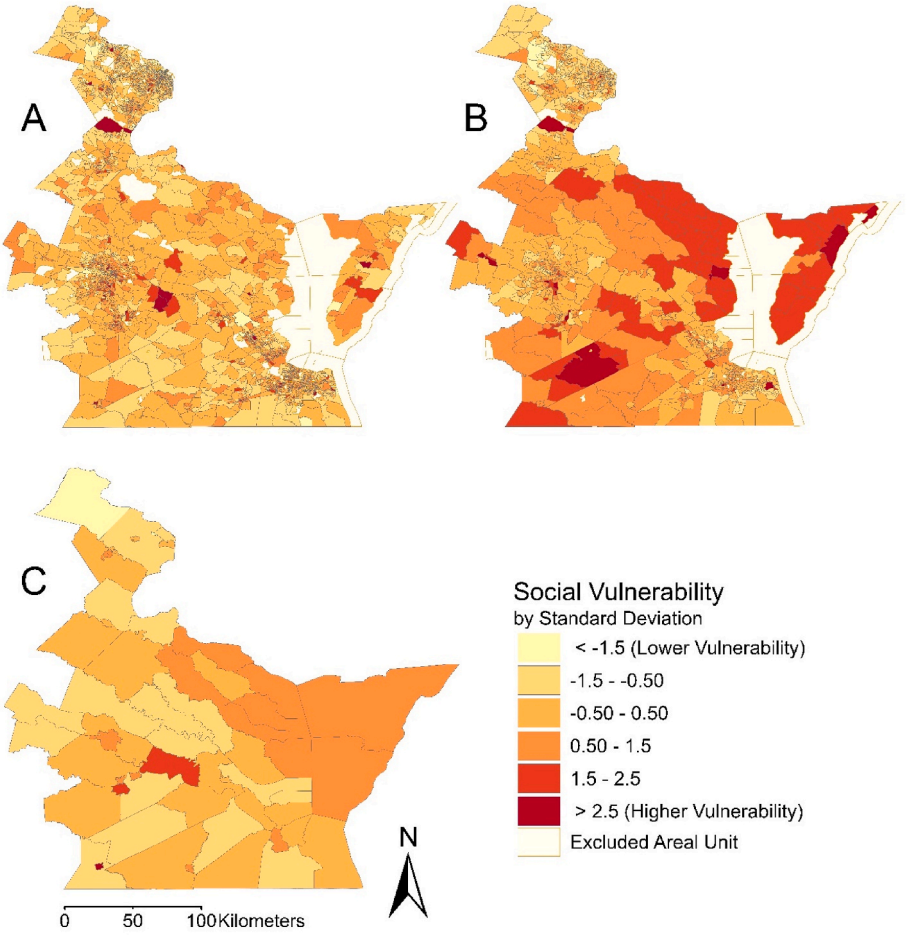

Fig. 4. The SoVI spatial distribution at the (a) BG, (b) tract, and (c) county scale. Each map contains six classes based on a standard deviation classification, which are very low (<-1.5), low (−1.5 to −0.5), low-medium (−0.5 – 0.5), medium-high (0.5–1.5), high (1.5–2.5), and very high (>2.5) social vulnerability. The areas excluded due to insufficient data are highlighted.

vulnerable communities within such target locations, at the magnitude of hundreds of thousands of people, is concerning from a methodological and flood risk management perspective (Fig. 8 Panel A). Likewise, the clusters and outliers account for variable trends in population density (Fig. 8 Panel B). Mixed spatial density trends within the bivariate extremes of H-L and L-H outliers depict opposing trends across scales. However, H–H clusters present primarily low population density, and L-L clusters contain highly populated regions. For example, the average population density across L-L clusters is 1.1 million people per sq. Mile. See Supplementary Section S.9 for not statistically significant and total count between scales, the relative number of aggregated units, and average HEMs and SoVIs values.

3.4. Indicator variability of flood exposure and social vulnerability clusters and outliers

The percent change between the indicators averages within coastal VA against the H–H, L-L, H-L, and L-H spatial clusters were calculated to understand how the social vulnerability indicators varied with flood exposure throughout scale (Supplementary Section S.10 Tables S10a, S10b, S10c, S10d). This investigative approach follows Tate et al., 2021. Outcomes reveal that the landscape of flood risk based on the LISA analysis reveals somewhat consistent but diverging trends, which could impact the strategy of flood resiliency approaches implemented. For example, in areas of H–H, consistent themes across scales include an increase, relative to the averages of coastal VA, in limited education, mobility challenges, lower income, and a decrease in Asian populations (Supplementary Table S10a). However, the influence of distinguishing indicators moving into H–H clusters is, for example, the percent change of mobile homes at the tract (213%) and county (232%) scale, which depicts a different geography of vulnerability at the BG scale (21%). Contradictory indicators such as language barriers where there is a negative percent change of at the BG (−45.1) and tract (−36.0), compared to a positive percent change at the county scale (51.3%). See supplementary section S.10 for a detailed analysis of the remaining spatial clusters (L-L, H-L, and L-H).

3.5. Variability of spatial autocorrelation across scale

The global Moran's I statistics for the SoVIs, HEMs, and the clusters and outliers of HEMs surrounded by SoVIs present variable trends for spatial autocorrelation (Table 2, see supplementary section S.11 for the Moran's scatterplots, LISA cluster maps, and statistical significance maps). Moran's I statistics for HEMs show a decrease as the level of aggregation increases. However, the opposite is true for the univariate SoVIs and bivariate HEMs and SoVIs.

4. Discussion

4.1. Variability of social vulnerability characteristics across scale

Our research found that the choice of spatial scale for data aggregation considerably impacts the correlation of social vulnerability indicators across Coastal VA, thus showing the effect of the MAUP. As

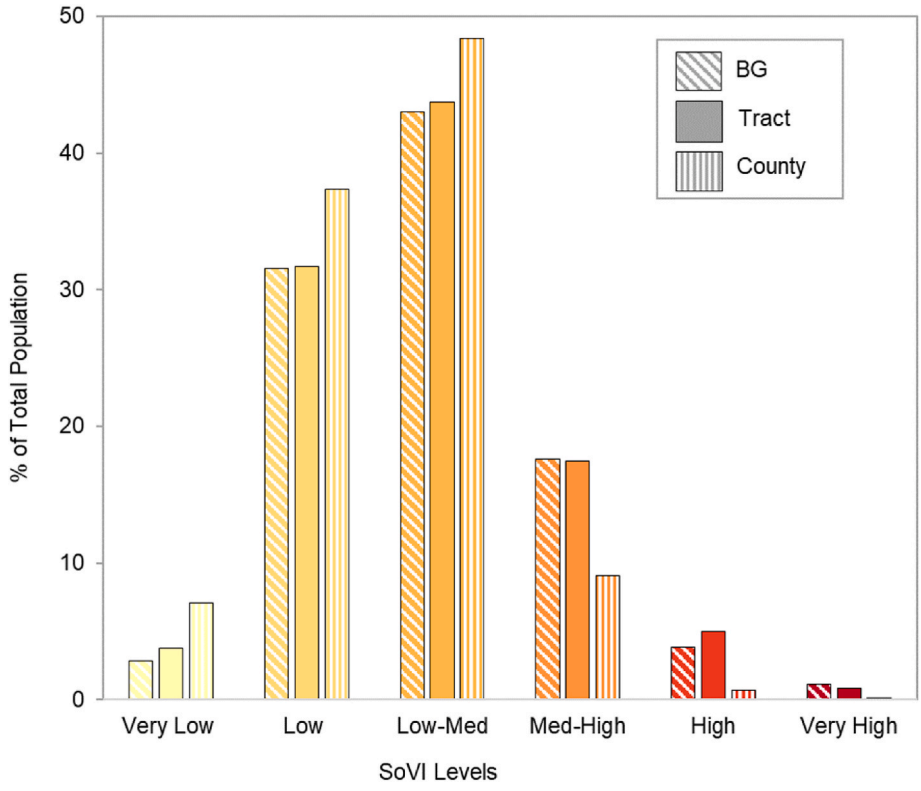

Fig. 5. The percent of the total population accounted for at varying levels of social vulnerability (based on one standard deviation) at the BG, tract, and county scale.

elaborated on by Chu et al., 2021, Census data is a non-modifiable entity that does not change temporally within a specific year (Chu et al., 2021). Therefore, the correlation of the indicators used for the SoVI creation was expected to be identical across scales. However, to an extent, similar themes of vulnerability are apparent across scales, such as low income and wealth, lack of transportation, vulnerable family structures, and young children and elderly populations, these results present similar themes within literature (see Kleinosky et al., 2007 and VA Dept. of Cons. and Rec, 2021) (Supplementary Section S.8 tables S8a, S8b, and S8c). Analogous to Schmidtlein et al., 2008, this result suggests that the effect of scale does not hinder the identification of significant drivers of vulnerability. However, arguably of most interest are indicators that are not consistent across scales with the SoVI measures, such as vacant households, Asian populations, and unemployed populations that are highly prevalent at one spatial scale and not as influential at another. This further confirms a conclusion made by Spielman et al., 2020 that the SoVI lacks internal consistency, which presents doubt in interpreting how valid this measurement scheme is in explaining social vulnerability and confirms calls to the sensitivity of the indicators (Spielman et al., 2020). Counter to previous scholarship, we found that the SoVI algorithm is not robust to minor changes in indicator selection and the level of aggregation (Schmidtlein et al., 2008).

4.2. Scale selection influence on social vulnerability identification

Through this study, we found that the number of PCs used for the SoVI creation and percent variance is contingent on scale selection. The BG and tract scales presented less percent variance than the county scale. Within the MAUP literature, percent variance is expected to decrease with increased aggregation (Prouse et al., 2014) due to a smoothing process of data extremes that occurs at greater spatial scales, which is indicative of information loss and generalization (Fotheringham & Wong, 1991; Openshaw & Taylor, 1979; Wong, 1996). However, a multi-scale SoVI comparison for South Carolina at the tract and county level showed increased percent variance with increased aggregation (Schmidtlein et al., 2008). Schmidtlein et al. rationalized the result given that the original construction of the "hazard-of-place" SoVI model was designed for the county scale, which presents two viewpoints of the SoVI results. Nonetheless, this result indicates that the SoVI model lacks internal consistency, which is imperative for a measurement instrument (Spielman et al., 2020).

Additionally, our results are consistent with other multi-scale studies (Remo et al., 2016; Tanir et al., 2021) that found that highly socially vulnerable residents were better detected at finer spatial scales than at coarser scales. In other words, if this study had been performed only at the county scale, the SoVI would have underreported a substantial number of people classified as highly vulnerable. However, there are contrasting results for vulnerability within the same spatial area across scales, which is a real problem brought on by the MAUP and influenced by the original Census data, which is also highlighted by a cross-scale study on social resilience (Chu et al., 2021). Therefore, understanding the extent to which scale affects the subsequent decision-making for resource allocation and risk-management strategies for priority populations within SoVI analysis is warranted as the MAUP can manifest itself into real-life consequences for people (Buzzelli, 2020).

4.3. The landscape of flood hazard exposure and social vulnerability

A key contribution of this study is highlighting the effect scale selection has on hotspot identification for the spatial relationship of flood exposure and social vulnerability. We found inconsistencies between the bivariate LISA maps and the degree of spatial autocorrelations which suggests that the scale effect is prevalent in flood vulnerability risk assessments. The prevalence of the scale effect can impact the identification of priority areas for flood risk reduction strategies. Generally, mitigation strategies are implemented at the county or jurisdictional level (Frazier et al., 2013; Remo et al., 2013). However, our research demonstrates the possibility of overlooking highly vulnerable populations at greater aggregated spatial scales (county) in flood vulnerability analyses – echoing other multi-scale flood vulnerability studies

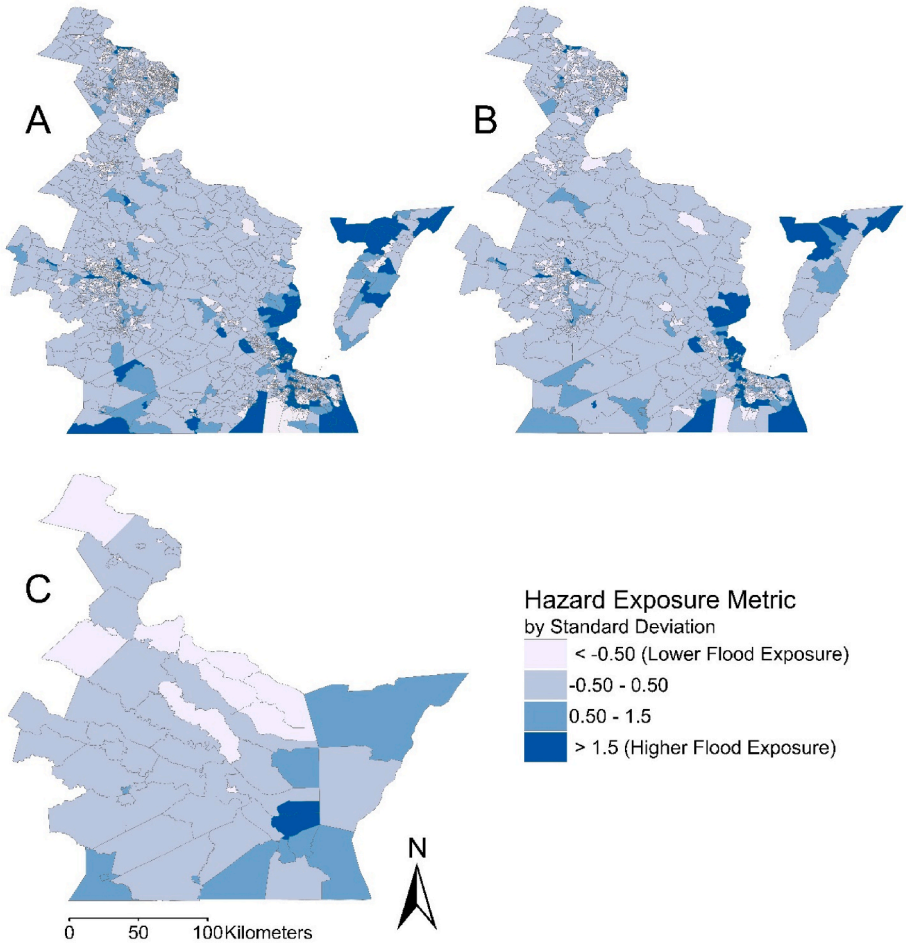

Fig. 6. The HEMs at the (a) BG, (b) tract, and (c) county scale.

(Remo et al., 2016; Tanir et al., 2021). As seen in Fig. 4, dense urban areas can vastly shift socioeconomic and demographic characteristics over a landscape; therefore, it is integral to consider how the selection of scale serves the flood risk mitigation strategies and the study area type. To avoid the ethical pitfalls of the ecological fallacy encountered when utilizing aggregated data (Alker, 1969; Clark & Avery, 1976), our work suggests the importance of including multi-scale analyses to reduce incorrect multilevel inferences made based on a single scale.

4.4. Spatial structure shifts across scales

As a result of this work, we found that scale selection based on the aggregated data plays a part in spatial association patterns. Generally, spatial autocorrelation is expected to decrease with increased aggregation (Y. H. Chou, 1991; Y.-H. Chou, 1995; Qi & Wu, 1996; Xu et al., 2017). Xu et al., 2017 described this as scale synthesis, which imitates a peak-cutting and valley-filling process, where smaller and isolated high values (H–H hot spots) or low values (L-L hot spots) are replaced or cut at increased aggregated scales. The Moran's I statistics for HEMs were found to be consistent with MAUP literature, however, an opposing trend was revealed for univariate SoVIs and bivariate HEMs and SoVIs. We interpret that given that the global Moran's I statistics are based on the contiguous spatial weight matrix, the increased null SoVI values at the BG level could have impacted the resulting spatial structure and trend, which is a similar inference by Chu et al., 2021.

4.5. Implications of scale on researcher approach and implementation

What implications does this raise for research methodological approaches? As described by Buzzelli, 2020, it is incorrect to assume that more minor aggregated spatial scales more closely represent what is occurring at the ground level than larger spatial scales (Buzzelli, 2020). There are tradeoffs with increased variability at smaller scales and increased generalization due to a smoothing effect occurring at larger spatial scales - highlighting why the effects of the MAUP is still an area of high inquiry within many topic areas of literature (for e.g., Barnes et al., 2016; Zhang et al., 2022). However, the tradeoff of increased variability presents to be a safer alternative than not accounting for highly vulnerable and flood-exposed communities. Additionally, a multi-scale social vulnerability or flood risk analysis may not be achievable across all organizations, such as local governments with limited resources and capacity (Burnstein & Rogin, 2022). Based on the results of this work within coastal VA, which we acknowledge could be variable across the study area, we would recommend that a smaller aggregated scale with minimal data loss be utilized for flood risk and social vulnerability analysis. For Coastal VA, we would advise Census tracts for flood vulnerability analysis based on the explained variance and overall data quality. The tract scale offers minimal data loss with greater spatial detail than the BG or county scales.

4.6. Limitations and future work

A few inherent limitations exist in this study's creation and point to future directions for research. First, we choose equal weighting of PCs to quantify vulnerability scores with the SoVI. This subjective choice weighs the dominant loading factor with high variance as equivalent to low percent variance factor loadings, altering our SoVI understandings. Second, the additive method is based on our interpretation of the

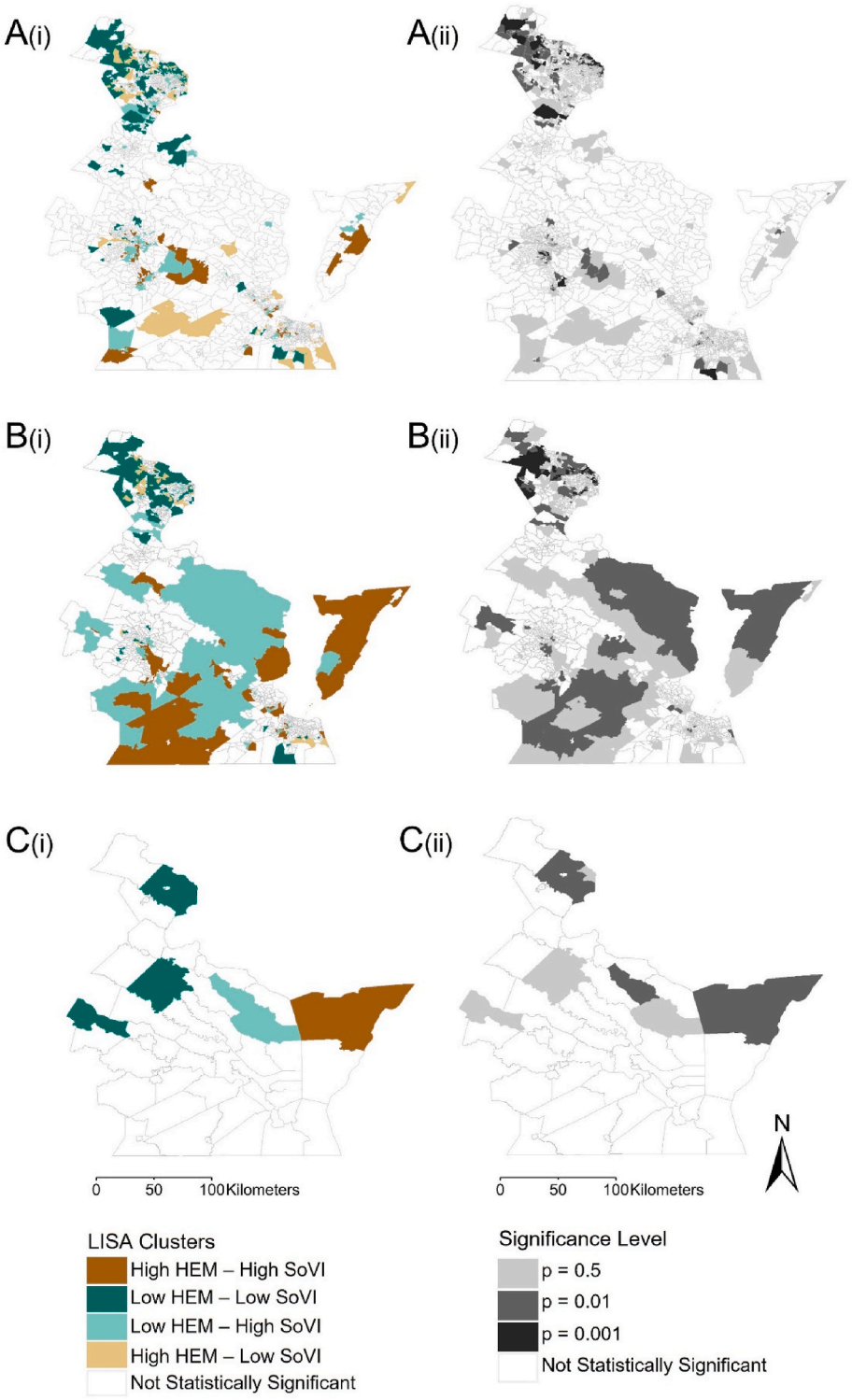

Fig. 7. Bivariate LISA (i) cluster maps and (ii) cluster significance maps of HEM surrounded by SoVI at the (a) BG, (b) tract, and (c) county scale.

indicators' influence on vulnerability. Therefore, the divergent SoVI results could be a combination of the PCA method approaches and the MAUP effects. Third, there was a lack of data quality accompanying the Census ACS data (King, 2001). Inconsistent missing data and gaps are a challenge in vulnerability assessments. We observed significant data gaps by validating the Census data used for this study. For example, we found a case in which 2018, 2019, and 2020 ACS 5-year estimates accounted for 7, 0, and 238 mobile homes, respectively, over a three-year survey period. As such, large variations such as these produce data gaps and inconsistencies that hinder the ability to understand the extent to which the data loss is supplementing observed social vulnerability and flood exposure spatial analysis trends across scale versus the MAUP. Lastly, in quantifying flood exposure, although adequate for the desired motivation of this work, future studies could consider incorporating advanced flood exposure approaches and data sources. For example, see Huang and Wang (2020), that better account for the heterogeneity of population distribution within the floodplain at a micro-level. Researchers could also leverage the advancements made by

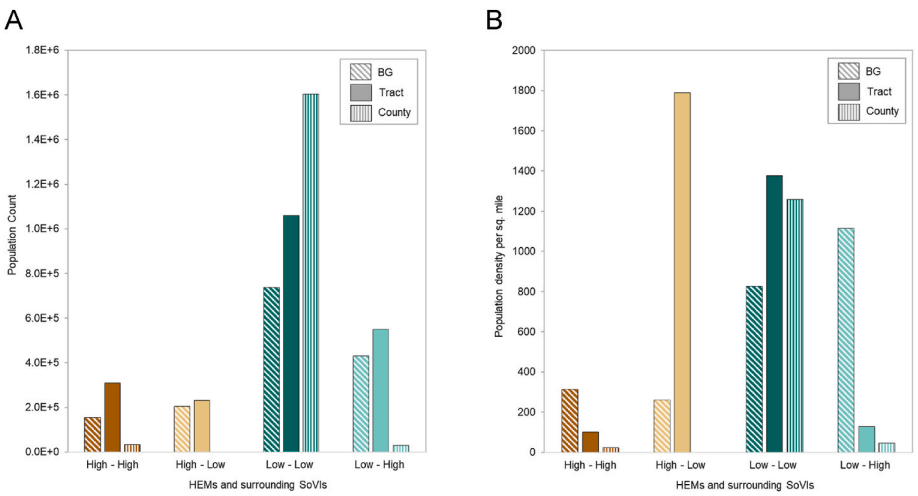

Fig. 8. (A) Population count and the (B) population density per sq. Mile for the bivariate LISA clusters at the BG, tract, and county scale.

Table 2
The univariate (SoVIs, HEMs) and bivariate (LISA hotspots) Moran's I by spatial scale. The global Moran's I is based on 999 permutations with a pseudo-significance level of $p \leq 0.05$.

Analysis Type	Spatial Scale	Global Moran's I	P-Value	Z-Value
Univariate Global Moran's I (SoVI)	BG	0.249	0.001	25.6
	Tract	0.444	0.001	28.5
	County	0.114	0.091	1.40
Univariate Global Moran's I (HEM)	BG	0.531	0.001	55.7
	Tract	0.433	0.001	26.2
	County	0.230	0.002	3.66
Bivariate Global Moran's I (HEM and SoVI)	BG	0.008	0.121	1.14
	Tract	0.096	0.001	8.19
	County	0.107	0.063	1.53

Flores et al. (2023) in dasymetric mapping using population density estimation within habitable areas. These approaches present promising opportunities to improve the accuracy of estimating populations exposed to flood hazards.

Future directions for this work could consider exploring the temporal and spatial aspects based on the new release of the 2020 Census. An exploration across data products could lend insight into data quality and further understanding of the effect of the MAUP on flood vulnerability quantification. Additionally, to our knowledge, all multi-scale flood vulnerability studies have been performed locally or at a single state level. There are only two U.S.-based multi-scale flood vulnerability studies that followed a similar approach to social vulnerability index creation with a divergent method of flood exposure and loss estimation through FEMA's Hazus-MH flood loss modeling software (Remo et al., 2016; Tanir et al., 2021). These flood vulnerability studies, along with this work, have been performed locally or at a single state level. Therefore, a national-based multi-scale flood vulnerability, potentially incorporating additional scales not explored in this work, such as block, jurisdictional, or state level, could lend insight into the heterogeneity of hotspots and outliers of flood exposure and social vulnerability within the continental US. Lastly, several indicator-based methodological approaches exist for quantifying social vulnerability to natural hazards, for example, see (CDC, 2020; Fitton et al., 2021), with contention on how to best measure vulnerability, such as indicator selection (Mavhura et al., 2017). There is a lack of studies that investigate not only how to measure the validity of such indices in practice (Bucherie et al., 2022) but also how the differences among the construction of current indices (e.g., spatial scale, indicators) impact decision-making for flood hazard management and adaptation. Further research is needed to bridge this gap and enhance our understanding of the quality and effectiveness of social vulnerability indices.

5. Conclusion

Our research highlights that scale selection matters in social vulnerability index and flood exposure metric creation. The vulnerability analysis showcased that scale influences the correlation of social vulnerability indicators. We found that there is not a consistent indicator across scales driving vulnerability; however, themes of economic inequities and mobility challenges transverse scales within coastal VA. This is an important finding as income and wealth are critical factors in determining how a household responds and recovers from a flood event (Gourevitch et al., 2022). Based on the choropleth mappings of the SoVIs, we found that greater aggregated scales overlooked areas of higher vulnerability detected at more minor aggregated scales. If used to inform flood mitigation policies and programs, it would further add to an inequitable landscape of flood risk.

The HEMs findings further demonstrated the effect of scale on summary values. The mean flood exposure shifts from 9.5, 10.3, and 12.2 percent at the BG, tract, and county scales. Like the SoVI analysis, choropleth mappings of HEMs identified areas of high flood exposure at smaller aggregated scales neglected at larger spatial scales. However, the patterns of flood exposure are generally mirrored throughout scale, detecting patterns of increased compound flooding towards the coast and upwards towards the Chesapeake Bay.

Based on the bivariate LISA, which identified hotspots and outliers of flood exposure (HEMs) surrounded by social vulnerability (SoVIs), we found that scale selection can highlight different priority areas for flood mitigation and risk reduction. For example, highly vulnerable areas with varying exposure – target locations for current and future flood risk reduction – accounted for hundreds of thousands more people at the BG and tract scale than at the county scale. Then by investigating the social vulnerability indicators associated with each cluster and outlier type, we found that the identified priority indicators of social vulnerability to high flood exposure in coastal VA vary with scale. Overall, this body of work contributes to the knowledge gap in understanding how the MAUP and selection of scale impact flood vulnerability results.

Funding source

Partial funding to support Selena Hinojos was provided by the National Science Foundation (NSF) under grant #1941657 and #2244715. Any opinions, findings, conclusions, or recommendations expressed in

this material do not necessarily reflect the view of the funding agency.

Data availability statement

Datasets for this research are openly available upon article acceptance at a permanent DOI database.

Declarations of interest

None.

Authors contribution

Selena Hinojos: Conceptualization, Methodology, Software, Formal analysis, Investigation, Data curation, Writing – original draft, Visualization. Caitlin Grady: Conceptualization, Methodology, Writing – review & editing, Supervision, Project administration, Funding acquisition. Peter Stempel: Writing - review & editing. Lauren McPhillips: Writing - review & editing.

Acknowledgments

The authors would like to acknowledge the National Science Foundation Grant #1941657 and #2244715, The Pennsylvania State University, and The George Washington University for supporting this work. The authors would also like to thank all the members of the FEWsLab, including Sarah Torhan, for their helpful suggestions.

Appendix A. Supplementary data

Supplementary data to this article can be found online at https://doi.org/10.1016/j.apgeog.2023.103017.

References

Abson, D. J., Dougill, A. J., & Stringer, L. C. (2012). Using principal component analysis for information-rich socio-ecological vulnerability mapping in southern africa. *Applied Geography, 35*(1), 515–524. https://doi.org/10.1016/j.apgeog.2012.08.004

Alker, H R (Ed.). (1969). *A typology of ecological fallacies. Quantitative Ecological Analysis in the Social Sciences* (pp. 69–86). Cambridge, MA: MIT Press.

Barnes, T. L., Colabianchi, N., Hibbert, J. D., Porter, D. E., Lawson, A. B., & Liese, A. D. (2016). Scale effects in food environment research: Implications from assessing socioeconomic dimensions of supermarket accessibility in an eight-county region of South Carolina. *Applied Geography, 68*, 20–27. https://doi.org/10.1016/j.apgeog.2016.01.004

Birkland, T. A., Burby, R. J., Conrad, D., Cortner, H., & Michener, W. K. (2003). River ecology and flood hazard mitigation. *Natural Hazards Review, 4*(1), 46–54. https://doi.org/10.1061/(ASCE)1527-6988(2003)4:1(46)

Blessing, R., Sebastian, A., & Brody, S. D. (2017). Flood risk delineation in the United States: How much loss are we capturing? *Natural Hazards Review, 18*(3), Article 04017002. https://doi.org/10.1061/(ASCE)NH.1527-6996.0000242

Bucherie, A., Hultquist, C., Adamo, S., Neely, C., Ayala, F., Bazo, J., & Kruczkiewicz, A. (2022). A comparison of social vulnerability indices specific to flooding in Ecuador: Principal component analysis (PCA) and expert knowledge. *International Journal of Disaster Risk Reduction, 73*, Article 102897. https://doi.org/10.1016/j.ijdrr.2022.102897

Bureau, U. C. (2020). *County population totals: 2010-2019*. Census.Gov. https://www.census.gov/data/tables/time-series/demo/popest/2010s-counties-total.html.

Burnstein, E., & Rogin, A. (2022). State flood resilience and adaptation planning: Challenges and opportunities. https://www.urban.org/research/publication/state-flood-resilience-and-adaptation-planning-challenges-and-opportunities.

Buzzelli, M. (2020). Modifiable areal unit problem. *International Encyclopedia of Human Geography*, 169–173. https://doi.org/10.1016/B978-0-08-102295-5.10406-8

CDC. (2020). CDC/ATSDR social vulnerability index (SVI). https://www.atsdr.cdc.gov/placeandhealth/svi/index.html.

Chakraborty, J., Collins, T. W., Montgomery, M. C., & Grineski, S. E. (2014). Social and spatial inequities in exposure to flood risk in miami, Florida. *Natural Hazards Review, 15*(3), Article 04014006. https://doi.org/10.1061/(ASCE)NH.1527-6996.0000140

Chou, Y. H. (1991). Map resolution and spatial autocorrelation. *Geographical Analysis, 23*(3), 228–246. https://doi.org/10.1111/j.1538-4632.1991.tb00236.x

Chou, Y.-H. (1995). Spatial pattern and spatial autocorrelation. In A. U. Frank, & W. Kuhn (Eds.), *Spatial information theory A theoretical basis for gis* (pp. 365–376). Springer. https://doi.org/10.1007/3-540-60392-1_24.

Chu, S. H. Y., Tan, S.-Y., & Mortsch, L. (2021). Social resilience to flooding in vancouver: The issue of scale. *Environmental Hazards, 20*(4), 400–415. https://doi.org/10.1080/17477891.2020.1834345

Clark, W.a. V., & Avery, K. L. (1976). The effects of data aggregation in statistical analysis. *Geographical Analysis, 8*(4), 428–438. https://doi.org/10.1111/j.1538-4632.1976.tb00549.x

Collins, T. W., Grineski, S. E., Chakraborty, J., & Flores, A. B. (2019). Environmental injustice and hurricane harvey: A household-level study of socially disparate flood exposures in greater houston, Texas, USA. *Environmental Research, 179*, Article 108772. https://doi.org/10.1016/j.envres.2019.108772

Crowell, M., Coulton, K., Johnson, C., Westcott, J., Bellomo, D., Edelman, S., & Hirsch, E. (2010). An estimate of the US population living in 100-year coastal flood hazard areas. *Journal of Coastal Research - J COASTAL RES, 26*. https://doi.org/10.2112/JCOASTRES-D-09-00076.1

Cutter, S. L., Boruff, B. J., & Shirley, W. L. (2003). Social vulnerability to environmental hazards. *Social Science Quarterly, 84*(2), 242–261. https://doi.org/10.1111/1540-6237.8402002

Debbage, N. (2019). Multiscalar spatial analysis of urban flood risk and environmental justice in the Charlanta megaregion, USA. *Anthropocene, 28*, Article 100226. https://doi.org/10.1016/j.ancene.2019.100226

Fekete, A., Damm, M., & Birkmann, J. (2010). Scales as a challenge for vulnerability assessment. *Natural Hazards, 55*(3), 729–747. https://doi.org/10.1007/s11069-009-9445-5

FEMA. (2022). National flood hazard layer. https://www.fema.gov/flood-maps/national-flood-hazard-layer.

Fitton, J. M., O'Dwyer, B., & Maher, B. (2021). Developing a social vulnerability to environmental hazards index to inform climate action in Ireland. *Irish Geography, 54*(2). Article 2.

Flores, A. B., Collins, T. W., Grineski, S. E., Amodeo, M., Porter, J. R., Sampson, C. C., & Wing, O. (2023). Federally overlooked flood risk inequities in houston, Texas: Novel insights based on dasymetric mapping and state-of-the-art flood modeling. *Annals of the Association of American Geographers, 113*(1), 240–260. https://doi.org/10.1080/24694452.2022.2085656

Fotheringham, A. S., & Wong, D. W. S. (1991). The modifiable areal unit problem in multivariate statistical analysis. *Environment and Planning: Economy and Space, 23*(7), 1025–1044. https://doi.org/10.1068/a231025

Frazier, T. G., Walker, M. H., Kumari, A., & Thompson, C. M. (2013). Opportunities and constraints to hazard mitigation planning. *Applied Geography, 40*, 52–60. https://doi.org/10.1016/j.apgeog.2013.01.008

Gourevitch, J. D., Diehl, R. M., Wemple, B. C., & Ricketts, T. H. (2022). Inequities in the distribution of flood risk under floodplain restoration and climate change scenarios. *People and Nature, 4*(2), 415–427. https://doi.org/10.1002/pan3.10290

Gu, H., Du, S., Liao, B., Wen, J., Wang, C., Chen, R., & Chen, B. (2018). A hierarchical pattern of urban social vulnerability in Shanghai, China and its implications for risk management. *Sustainable Cities and Society, 41*, 170–179. https://doi.org/10.1016/j.scs.2018.05.047

Hazards and Vulnerability Research Institute. (2015). HVRI. *SoVI®: Social vulnerability Index for the United States-2010–2014*. https://www.sc.edu/study/colleges_schools/artsandsciences/centers_and_institutes/hvri/index.php/sovi%c2%ae-0.

Hotelling, H. (1933). Analysis of a complex of statistical variables into principal components. *Journal of Educational Psychology, 24*(6), 417–441. https://doi.org/10.1037/h0071325

Huang, X., & Wang, C. (2020). Estimates of exposure to the 100-year floods in the conterminous United States using national building footprints. *International Journal of Disaster Risk Reduction, 50*, Article 101731. https://doi.org/10.1016/j.ijdrr.2020.101731

HVRI. (2016). *The SoVI® recipe—college of arts and sciences*. University of South Carolina. https://sc.edu/study/colleges_schools/artsandsciences/centers_and_institutes/hvri/data_and_resources/sovi/sovi_recipe/index.php.

Khajehei, S., Ahmadalipour, A., Shao, W., & Moradkhani, H. (2020). A place-based assessment of flash flood hazard and vulnerability in the contiguous United States. *Scientific Reports, 10*(1). https://doi.org/10.1038/s41598-019-57349-z. Article 1.

King, D. (2001). Uses and limitations of socioeconomic indicators of community vulnerability to natural hazards: Data and disasters in northern Australia. *Natural Hazards, 24*(2), 147–156. https://doi.org/10.1023/A:1011859507188

Kleinosky, L. R., Yarnal, B., & Fisher, A. (2007). Vulnerability of Hampton Roads, Virginia to storm-surge flooding and sea-level rise. *Natural Hazards, 40*(1), 43–70. https://doi.org/10.1007/s11069-006-0004-z

Linscott, G., Rishworth, A., King, B., & Hiestand, M. P. (2022). Uneven experiences of urban flooding: Examining the 2010 Nashville flood. *Natural Hazards, 110*(1), 629–653. https://doi.org/10.1007/s11069-021-04961-w

de Loyola Hummell, B. M., Cutter, S. L., & Emrich, C. T. (2016). Social vulnerability to natural hazards in Brazil. *International Journal of Disaster Risk Science, 7*(2), 111–122. https://doi.org/10.1007/s13753-016-0090-9

Maantay, J., & Maroko, A. (2009). Mapping urban risk: Flood hazards, race, & environmental justice in New York. *Applied Geography, 29*(1), 111–124. https://doi.org/10.1016/j.apgeog.2008.08.002

Mavhura, E., Manyena, B., & Collins, A. (2017). An approach for measuring social vulnerability in context: The case of flood hazards in Muzarabani district, Zimbabwe. *Geoforum, 86*, 103–117. https://doi.org/10.1016/j.geoforum.2017.09.008

Mazumder, L. T., Landry, S., & Alsharif, K. (2022). Coastal cities in the Southern US floodplains: An evaluation of environmental equity of flood hazards and social vulnerabilities. *Applied Geography, 138*, Article 102627. https://doi.org/10.1016/j.apgeog.2021.102627

Montgomery, M. C., & Chakraborty, J. (2013). Social vulnerability to coastal and inland flood hazards: A comparison of GIS-based spatial interpolation methods.

International Journal of Applied Geospatial Research, 4(3), 58–79. https://doi.org/10.4018/jagr.2013070104
NASEM (National Academies of Sciences, Engineering, and Medicine). (2019). Framing the challenge of urban flooding in the United States. https://doi.org/10.17226/25381.
NCEI. (2022). NOAA national centers for environmental information (NCEI) U.S. Billion-dollar weather and climate disasters. https://doi.org/10.25921/stkw-7w73.
NLCD. (2019). Multi-resolution land characteristics (MRLC) consortium national land cover database. https://www.mrlc.gov/data.
NOAA. (2023). Hampton Roads' sea level rise adaptation advances on multiple fronts. https://coast.noaa.gov/states/stories/sea-level-rise-adaptation-advances-on-multiple-fronts.html#.
Openshaw, S. (1984). Ecological fallacies and the analysis of areal Census data. *Environment and Planning: Economy and Space, 16*(1), 17–31. https://doi.org/10.1068/a160017
Openshaw, S., & Taylor, P. (1979). A million or so correlation coefficients: Three experiments on the modifiable areal unit problem. *Statistical Applications in the Spatial Sciences*, 127–144.
Pearson, K. (1901). LIII. On lines and planes of closest fit to systems of points in space. *The London, Edinburgh and Dublin Philosophical Magazine and Journal of Science, 2*(11), 559–572. https://doi.org/10.1080/14786440109462720
Pricope, N. G., Halls, J. N., & Rosul, L. M. (2019). Modeling residential coastal flood vulnerability using finished-floor elevations and socio-economic characteristics. *Journal of Environmental Management, 237*, 387–398. https://doi.org/10.1016/j.jenvman.2019.02.078
Prouse, V., Ramos, H., Grant, J. L., & Radice, M. (2014). How and when scale matters: The modifiable areal unit problem and income inequality in halifax. *Canadian Journal of Urban Research, 23*(1), 61–82.
Qiang, Y. (2019a). Disparities of population exposed to flood hazards in the United States. *Journal of Environmental Management, 232*, 295–304. https://doi.org/10.1016/j.jenvman.2018.11.039
Qiang, Y. (2019b). Flood exposure of critical infrastructures in the United States. *International Journal of Disaster Risk Reduction, 39*, Article 101240. https://doi.org/10.1016/j.ijdrr.2019.101240
Qiang, Y., Lam, N. S. N., Cai, H., & Zou, L. (2017). Changes in exposure to flood hazards in the United States. *Annals of the Association of American Geographers, 107*(6), 1332–1350. https://doi.org/10.1080/24694452.2017.1320214
Qi, Y., & Wu, J. (1996). Effects of changing spatial resolution on the results of landscape pattern analysis using spatial autocorrelation indices. *Landscape Ecology, 11*(1), 39–49. https://doi.org/10.1007/BF02087112
Rabby, Y. W., Hossain, M. B., & Hasan, M. U. (2019). Social vulnerability in the coastal region of Bangladesh: An investigation of social vulnerability index and scalar change effects. *International Journal of Disaster Risk Reduction, 41*, Article 101329. https://doi.org/10.1016/j.ijdrr.2019.101329
Remo, J. W. F., Pinter, N., & Mahgoub, M. (2016). Assessing Illinois's flood vulnerability using Hazus-MH. *Natural Hazards, 81*(1), 265–287. https://doi.org/10.1007/s11069-015-2077-z
Remo, J. W. F., Printer, N., Ellison, B., & Mahoub, M. (2013). Illinois statewide flood hazard assessment. In *Illinois emergency management agency, 2013 Illinois natural hazard mitigation plan*. http://www.illinois. gov/iema/Mitigation/documents/Plan_IllMitigationPlan.pdf.
Rufat, S., Tate, E., Emrich, C. T., & Antolini, F. (2019). How valid are social vulnerability models? *Annals of the Association of American Geographers, 109*(4), 1131–1153. https://doi.org/10.1080/24694452.2018.1535887
Schmidtlein, M. C., Deutsch, R. C., Piegorsch, W. W., & Cutter, S. L. (2008). A sensitivity analysis of the social vulnerability index. *Risk Analysis, 28*(4), 1099–1114. https://doi.org/10.1111/j.1539-6924.2008.01072.x
Schmidtlein, M. C., Shafer, J. M., Berry, M., & Cutter, S. L. (2011). Modeled earthquake losses and social vulnerability in Charleston, South Carolina. *Applied Geography, 31*(1), 269–281. https://doi.org/10.1016/j.apgeog.2010.06.001
Shao, W., Jackson, N. P., Ha, H., & Winemiller, T. (2020). Assessing community vulnerability to floods and hurricanes along the Gulf Coast of the United States. *Disasters, 44*(3), 518–547. https://doi.org/10.1111/disa.12383
Spielman, S. E., Tuccillo, J., Folch, D. C., Schweikert, A., Davies, R., Wood, N., & Tate, E. (2020). Evaluating social vulnerability indicators: Criteria and their application to the Social Vulnerability Index. *Natural Hazards, 100*(1), 417–436. https://doi.org/10.1007/s11069-019-03820-z
Strauss, B., Tebaldi, C., & Kulp, S. (2014). Virginia and the surging sea | surging seas: Sea level rise analysis by climate central. https://sealevel.climatecentral.org/research/reports/virginia-and-the-surging-sea.
Tanir, T., Sumi, S. J., Lima, A. de S., de, Coelho, G. de A., Uzun, S., Cassalho, F., & Ferreira, C. M. (2021). Multi-scale comparison of urban socio-economic vulnerability in the Washington, DC metropolitan region resulting from compound flooding. *International Journal of Disaster Risk Reduction, 61*, Article 102362. https://doi.org/10.1016/j.ijdrr.2021.102362
Tasnuva, A., Hossain, M. R., Salam, R., Islam, A. R. M. T., Patwary, M. M., & Ibrahim, S. M. (2020). *Employing social vulnerability index to assess household social vulnerability of natural hazards: An evidence from southwest coastal Bangladesh*. Environment, Development and Sustainability. https://doi.org/10.1007/s10668-020-01054-9
Tate, E. (2013). Uncertainty analysis for a social vulnerability index. *Annals of the Association of American Geographers, 103*(3), 526–543. https://doi.org/10.1080/00045608.2012.700616
Tate, E., Rahman, M. A., Emrich, C. T., & Sampson, C. C. (2021). Flood exposure and social vulnerability in the United States. *Natural Hazards, 106*(1), 435–457. https://doi.org/10.1007/s11069-020-04470-2
US Census Bureau. (2019). *American community survey (ACS)*. Census.Gov. https://www.census.gov/programs-surveys/acs.
US EPA, O.. (2015). Dasymetric toolbox [Data and Tools] https://www.epa.gov/enviroatlas/dasymetric-toolbox.
VA Dept. of Cons. and Rec. (2021). Virginia coastal resilience master plan. https://www.dcr.virginia.gov/crmp/plan#plan.
Walker, H. (2022). Tidycensus: Load US Census Boundary and attribute Data as "tidyverse" and 'sf'-ready data frames. *R package version 1.1.9*.9000 https://walker-data.com/tidycensus/.
Wang, Y. V., & Sebastian, A. (2021). Community flood vulnerability and risk assessment: An empirical predictive modeling approach. *Journal of Flood Risk Management, 14*(3), Article e12739. https://doi.org/10.1111/jfr3.12739
Wang, C., & Yarnal, B. (2012). The vulnerability of the elderly to hurricane hazards in Sarasota, Florida. *Natural Hazards, 63*(2), 349–373. https://doi.org/10.1007/s11069-012-0151-3
Wing, O. E. J., Bates, P. D., Smith, A. M., Sampson, C. C., Johnson, K. A., Fargione, J., & Morefield, P. (2018). Estimates of present and future flood risk in the conterminous United States. *Environmental Research Letters, 13*(3), Article 034023. https://doi.org/10.1088/1748-9326/aaac65
Wong, D. (1996). Aggregation effects in geo-referenced data. In *PRACTICAL HANDBOOK of spatial statistics*. CRC Press.
Xu, S., Liu, Y., Wang, X., & Zhang, G. (2017). Scale effect on spatial patterns of ecosystem services and associations among them in semi-arid area: A case study in ningxia hui autonomous region, China. *The Science of the Total Environment, 598*, 297–306. https://doi.org/10.1016/j.scitotenv.2017.04.009
Yager, J., & Rosoff, S. (2017). Population in the U.S. Floodplains. https://furmancenter.org/research/publication/population-in-the-us-floodplains.
Zhang, S., Wang, M., Yang, Z., & Zhang, B. (2022). Do spatiotemporal units matter for exploring the microgeographies of epidemics? *Applied Geography, 142*, Article 102692. https://doi.org/10.1016/j.apgeog.2022.102692